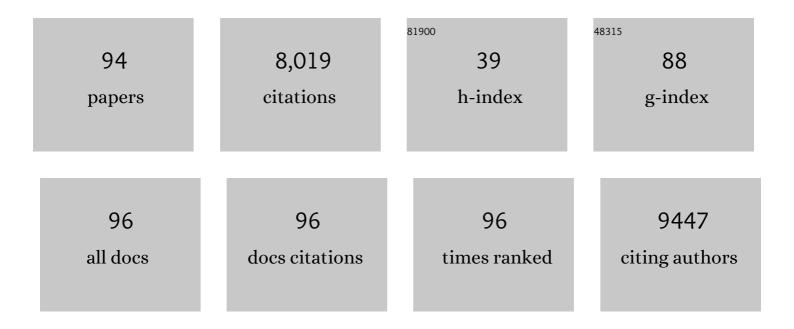
Jiangwei Wang

List of Publications by Year in descending order

Source: https://exaly.com/author-pdf/7751125/publications.pdf Version: 2024-02-01



#	Article	IF	CITATIONS
1	Solvent sieving separators implement dual electrolyte for high-voltage lithium-metal batteries. Nano Research, 2023, 16, 4901-4907.	10.4	4
2	Discrete twinning dynamics and size-dependent dislocation-to twin transition in body-centred cubic tungsten. Journal of Materials Science and Technology, 2022, 106, 33-40.	10.7	19
3	Atomic-scale study on the precipitation behavior of an Al–Zn–Mg–Cu alloy during isochronal aging. Journal of Materials Science and Technology, 2022, 108, 281-292.	10.7	15
4	A geometrical model for grain boundary migration mediated formation of multifold twins. International Journal of Plasticity, 2022, 148, 103128.	8.8	12
5	Bichannel design inspired by membrane pump: a rate booster for the conversion-type anode of sodium-ion battery. Journal of Materials Chemistry A, 2022, 10, 3373-3381.	10.3	2
6	Combined effect of Sn addition and pre-ageing on natural secondary and artificial ageing of Al–Mg–Si alloys. Journal of Materials Science, 2022, 57, 2149-2162.	3.7	3
7	Twin-coupled shear bands in an ultrafine-grained CoCrFeMnNi high-entropy alloy deformed at 77K. Materials Research Letters, 2022, 10, 385-391.	8.7	14
8	Atomistic dynamics of disconnection-mediated grain boundary plasticity: A case study of gold nanocrystals. Journal of Materials Science and Technology, 2022, 125, 182-191.	10.7	9
9	Shock-induced α" martensitic transformation in Nb single crystals. Materials Science & Engineering A: Structural Materials: Properties, Microstructure and Processing, 2022, 846, 143274.	5.6	7
10	Hierarchical twinning governed by defective twin boundary in metallic materials. Science Advances, 2022, 8, .	10.3	33
11	Mechanical Properties and Fracture Behavior of Laser Powder-Bed-Fused GH3536 Superalloy. Metals, 2022, 12, 1165.	2.3	3
12	Fatigue-induced interface damage in Cu/V nanoscale metallic multilayers. Scripta Materialia, 2021, 190, 103-107.	5.2	8
13	Long-term degradation behavior of slurry aluminide coating on Super304H stainless steel at 650â€ [~] °C. Corrosion Science, 2021, 178, 109054.	6.6	7
14	Sandwich structure stabilized atomic Fe catalyst for highly efficient Fenton-like reaction at all pH values. Applied Catalysis B: Environmental, 2021, 282, 119551.	20.2	93
15	Combined quantum tunnelling and dielectrophoretic trapping for molecular analysis at ultra-low analyte concentrations. Nature Communications, 2021, 12, 913.	12.8	34
16	Inclination-governed deformation of dislocation-type grain boundaries. Journal of Materials Research, 2021, 36, 1306-1315.	2.6	2
17	Defect-free potassium manganese hexacyanoferrate cathode material for high-performance potassium-ion batteries. Nature Communications, 2021, 12, 2167.	12.8	153
18	Metal–Organic Framework@Polyacrylonitrile-Derived Potassiophilic Nanoporous Carbon Nanofiber Paper Enables Stable Potassium Metal Anodes. ACS Applied Energy Materials, 2021, 4, 6245-6252.	5.1	23

#	Article	IF	CITATIONS
19	Diffusive crack-grain interplay in freestanding nanocrystalline silver thin film. Materialia, 2021, 17, 101116.	2.7	1
20	A comprehensive investigation of phase evolution of Al-Si coating during the prolonged aging at 650 ŰC. Corrosion Science, 2021, 189, 109605.	6.6	6
21	Coordinated grain boundary deformation governed nanograin annihilation in shear cycling. Journal of Materials Science and Technology, 2021, 86, 180-191.	10.7	14
22	Revealing extreme twin-boundary shear deformability in metallic nanocrystals. Science Advances, 2021, 7, eabe4758.	10.3	46
23	Penta-Twin Destruction by Coordinated Twin Boundary Deformation. Nano Letters, 2021, 21, 8378-8384.	9.1	10
24	Defect-driven selective metal oxidation at atomic scale. Nature Communications, 2021, 12, 558.	12.8	47
25	High-performance layered potassium vanadium oxide for K-ion batteries enabled by reduced long-range structural order. Journal of Materials Chemistry A, 2021, 9, 13125-13134.	10.3	17
26	Directing the deposition of lithium metal to the inner concave surface of graphitic carbon tubes to enable lithium-metal batteries. Journal of Materials Chemistry A, 2021, 9, 16936-16942.	10.3	5
27	Shear band mediated ω phase transformation in Nb single crystals deformed at 77 K. Materials Research Letters, 2021, 9, 523-530.	8.7	10
28	Sulfurized Polyacrylonitrile as a High-Performance and Low-Volume Change Anode for Robust Potassium Storage. ACS Nano, 2021, 15, 18419-18428.	14.6	17
29	Interactions between Dislocations and Penta-Twins in Metallic Nanocrystals. Metals, 2021, 11, 1775.	2.3	1
30	Twinning-assisted dynamic adjustment of grain boundary mobility. Nature Communications, 2021, 12, 6695.	12.8	23
31	Dualâ€Additive Assisted Chemical Vapor Deposition for the Growth of Mnâ€Doped 2D MoS ₂ with Tunable Electronic Properties. Small, 2020, 16, e1903181.	10.0	54
32	Confined seeds derived sodium titanate/graphene composite with synergistic storage ability toward high performance sodium ion capacitors. Chemical Engineering Journal, 2020, 379, 122418.	12.7	23
33	Plasmonic modulation of gold nanotheranostics for targeted NIR-II photothermal-augmented immunotherapy. Nano Today, 2020, 35, 100987.	11.9	55
34	Role of intersecting grain boundary on the deformation of twin-twin intersection. Scripta Materialia, 2020, 188, 184-189.	5.2	15
35	Free-Standing Two-Dimensional Gold Membranes Produced by Extreme Mechanical Thinning. ACS Nano, 2020, 14, 17091-17099.	14.6	15
36	Role of interfacial transition zones in the fracture of Cu/V nanolamellar multilayers. Materials Research Letters, 2020, 8, 299-306.	8.7	13

#	Article	IF	CITATIONS
37	A Nonflammable Electrolyte Enabled High Performance K _{0.5} MnO ₂ Cathode for Low-Cost Potassium-Ion Batteries. ACS Energy Letters, 2020, 5, 1916-1922.	17.4	61
38	Unstable twin in body-centered cubic tungsten nanocrystals. Nature Communications, 2020, 11, 2497.	12.8	40
39	High performance potassium–sulfur batteries and their reaction mechanism. Journal of Materials Chemistry A, 2020, 8, 10875-10884.	10.3	40
40	Anti-twinning in nanoscale tungsten. Science Advances, 2020, 6, eaay2792.	10.3	49
41	Metallic nanocrystals with low angle grain boundary for controllable plastic reversibility. Nature Communications, 2020, 11, 3100.	12.8	53
42	In situ atomistic observation of the deformation mechanism of Au nanowires with twin–twin intersection. Journal of Materials Science and Technology, 2020, 53, 118-125.	10.7	19
43	Size-dependent dislocation–twin interactions. Nanoscale, 2019, 11, 12672-12679.	5.6	28
44	Local lattice distortion mediated formation of stacking faults in Mg alloys. Acta Materialia, 2019, 170, 231-239.	7.9	45
45	Growth of environmentally stable transition metal selenide films. Nature Materials, 2019, 18, 602-607.	27.5	116
46	Formation of mixed metal sulfides of NixCu1â^'xCo2S4 for high-performance supercapacitors. Journal of Electroanalytical Chemistry, 2019, 836, 134-142.	3.8	35
47	Bending-induced deformation twinning in body-centered cubic tungsten nanowires. Materials Research Letters, 2019, 7, 210-216.	8.7	29
48	In situ atomistic observation of disconnection-mediated grain boundary migration. Nature Communications, 2019, 10, 156.	12.8	98
49	Deformation-induced interfacial transition zone in Cu/V nanolamellar multilayers. Scripta Materialia, 2019, 159, 104-108.	5.2	17
50	Enhancing the Strength of Graphene by a Denser Grain Boundary. ACS Nano, 2018, 12, 4529-4535.	14.6	39
51	Harnessing the concurrent reaction dynamics in active Si and Ge to achieve high performance lithium-ion batteries. Energy and Environmental Science, 2018, 11, 669-681.	30.8	329
52	Free-Standing Nitrogen-Doped Cup-Stacked Carbon Nanotube Mats for Potassium-Ion Battery Anodes. ACS Applied Energy Materials, 2018, 1, 1703-1707.	5.1	90
53	Discrete shear band plasticity through dislocation activities in body-centered cubic tungsten nanowires. Scientific Reports, 2018, 8, 4574.	3.3	22
54	Design principle of all-inorganic halide perovskite-related nanocrystals. Journal of Materials Chemistry C, 2018, 6, 12484-12492.	5.5	38

#	Article	IF	CITATIONS
55	Superplasticity in Cold Nanowires through the Operation of Multiple Slip Systems. Advanced Functional Materials, 2018, 28, 1805258.	14.9	21
56	Consecutive crystallographic reorientations and superplasticity in body-centered cubic niobium nanowires. Science Advances, 2018, 4, eaas8850.	10.3	46
57	Mechanical property of metallic nanowires: the shorter is stronger and ductile. Materials Science & Engineering A: Structural Materials: Properties, Microstructure and Processing, 2018, 733, 164-169.	5.6	13
58	Dispersion-strengthened microparticle silicon composite with high anti-pulverization capability for Li-ion batteries. Energy Storage Materials, 2018, 14, 279-288.	18.0	45
59	Atomic-scale mechanism of the Î,â€3 → Î,â€2 phase transformation in Al-Cu alloys. Journal of Materials Science and Technology, 2017, 33, 1159-1164.	10.7	63
60	Hydrothermal synthesis and formation mechanism of single-crystal Auivillius Bi4Ti3O12 nanosheets with ammonium bismuth citrate (C6H10BiNO8) as Bi sources. Journal of Crystal Growth, 2017, 476, 31-37.	1.5	10
61	Reaction and Capacity-Fading Mechanisms of Tin Nanoparticles in Potassium-Ion Batteries. Journal of Physical Chemistry C, 2017, 121, 12652-12657.	3.1	150
62	Improved Na-storage cycling of amorphous-carbon-sheathed Ni3S2 arrays and investigation by in situ TEM characterization. Materials Today Energy, 2017, 5, 99-106.	4.7	22
63	High rate and long cycle life porous carbon nanofiber paper anodes for potassium-ion batteries. Journal of Materials Chemistry A, 2017, 5, 19237-19244.	10.3	195
64	Tuning the Outward to Inward Swelling in Lithiated Silicon Nanotubes via Surface Oxide Coating. Microscopy and Microanalysis, 2017, 23, 2018-2019.	0.4	0
65	Highly-efficient MnO2/carbon array-type catalytic cathode enabling confined Li2O2 growth for long-life Li–O2 batteries. Energy Storage Materials, 2017, 6, 164-170.	18.0	27
66	Olivine LiFePO4 nanocrystallites embedded in carbon-coating matrix for high power Li-ion batteries. Electrochimica Acta, 2016, 222, 685-692.	5.2	30
67	Ethylene glycol (EG) solvothermal synthesis of flower-like LiMnPO ₄ nanostructures self-assembled with (010) nanobelts for Li-ion battery positive cathodes. CrystEngComm, 2016, 18, 3282-3288.	2.6	18
68	In situ nanomechanical testing of twinned metals in a transmission electron microscope. MRS Bulletin, 2016, 41, 305-313.	3.5	13
69	Tuning the Outward to Inward Swelling in Lithiated Silicon Nanotubes via Surface Oxide Coating. Nano Letters, 2016, 16, 5815-5822.	9.1	45
70	Atomistic perspective on in situ nanomechanics. Extreme Mechanics Letters, 2016, 8, 127-139.	4.1	29
71	Hydrothermal synthesis and formation mechanism of the single-crystalline Bi ₄ Ti ₃ O ₁₂ nanosheets with dominant (010) facets. CrystEngComm, 2016, 18, 2268-2274.	2.6	38
72	Size-Dependent Brittle-to-Ductile Transition in Silica Glass Nanofibers. Nano Letters, 2016, 16, 105-113.	9.1	120

#	Article	IF	CITATIONS
73	In situ atomic-scale observation of twinning-dominated deformation in nanoscale body-centred cubic tungsten. Nature Materials, 2015, 14, 594-600.	27.5	250
74	Nanoscale origins of the damage tolerance of the high-entropy alloy CrMnFeCoNi. Nature Communications, 2015, 6, 10143.	12.8	608
75	Nanoscale Deformation Analysis With High-Resolution Transmission Electron Microscopy and Digital Image Correlation. Journal of Applied Mechanics, Transactions ASME, 2015, 82, .	2.2	26
76	Tailoring Pore Size of Nitrogenâ€Đoped Hollow Carbon Nanospheres for Confining Sulfur in Lithium–Sulfur Batteries. Advanced Energy Materials, 2015, 5, 1401752.	19.5	273
77	Hydrothermal synthesis of flower-like LiMnPO4nanostructures self-assembled with (010) nanosheets and their application in Li-ion batteries. CrystEngComm, 2015, 17, 6399-6405.	2.6	30
78	Strong Hall–Petch Type Behavior in the Elastic Strain Limit of Nanotwinned Gold Nanowires. Nano Letters, 2015, 15, 3865-3870.	9.1	41
79	High damage tolerance of electrochemically lithiated silicon. Nature Communications, 2015, 6, 8417.	12.8	96
80	Structural Evolution and Pulverization of Tin Nanoparticles during Lithiation-Delithiation Cycling. Journal of the Electrochemical Society, 2014, 161, F3019-F3024.	2.9	96
81	Void-assisted plasticity in Ag nanowires with a single twin structure. Nanoscale, 2014, 6, 9574.	5.6	28
82	Formation of monatomic metallic glasses through ultrafast liquid quenching. Nature, 2014, 512, 177-180.	27.8	365
83	Lithium–tellurium batteries based on tellurium/porous carbon composite. Journal of Materials Chemistry A, 2014, 2, 12201-12207.	10.3	121
84	In Situ Transmission Electron Microscopy Study of Electrochemical Sodiation and Potassiation of Carbon Nanofibers. Nano Letters, 2014, 14, 3445-3452.	9.1	263
85	Near-ideal theoretical strength in gold nanowires containing angstrom scale twins. Nature Communications, 2013, 4, 1742.	12.8	226
86	Two-Phase Electrochemical Lithiation in Amorphous Silicon. Nano Letters, 2013, 13, 709-715.	9.1	377
87	Study of the failure mechanism of an epoxy coating system under high hydrostatic pressure. Corrosion Science, 2013, 74, 59-70.	6.6	78
88	In situ atomic-scale imaging of electrochemical lithiation in silicon. Nature Nanotechnology, 2012, 7, 749-756.	31,5	533
89	Microstructural Evolution of Tin Nanoparticles during In Situ Sodium Insertion and Extraction. Nano Letters, 2012, 12, 5897-5902.	9.1	491
90	Sandwich-Lithiation and Longitudinal Crack in Amorphous Silicon Coated on Carbon Nanofibers. ACS Nano, 2012, 6, 9158-9167.	14.6	72

#	Article	IF	CITATIONS
91	Anisotropic Swelling and Fracture of Silicon Nanowires during Lithiation. Nano Letters, 2011, 11, 3312-3318.	9.1	691
92	Ultrafast Electrochemical Lithiation of Individual Si Nanowire Anodes. Nano Letters, 2011, 11, 2251-2258.	9.1	379
93	Lithiation-Induced Embrittlement of Multiwalled Carbon Nanotubes. ACS Nano, 2011, 5, 7245-7253.	14.6	122
94	Tensile Deformation Behaviors of CuNi Alloy Processed by Equal Channel Angular Pressing. Advanced Engineering Materials, 2010, 12, 304-311.	3.5	6